

## Emulating chatter with process damping in turning using a hardware-in-the-loop simulator

Govind N. Sahu<sup>\*[0000-0001-7722-4107]</sup>, Pulkit Jain<sup>[0000-0003-2600-773X]</sup>,  
Mohit Law<sup>[0000-0003-2659-4188]</sup> and Pankaj Wahi<sup>[0000-0003-2106-0881]</sup>

Department of Mechanical Engineering, Indian Institute of Technology Kanpur, Kanpur  
208016, India

\*govinds@iitk.ac.in

**Abstract.** Improved chatter vibration free cutting performance at low speeds occur due to process damping. An additional cutting force component that arises due to interference of the vibrating tool with the cut surface is thought to be responsible for this damping. Experimentally identifying and isolating the mechanisms causing process damping is difficult due to its complex relationship with tool wear. This paper hence proposes the use of a hardware-in-the-loop (HiL) simulator to investigate and emulate stability of turning with process damping. The HiL simulator has a hardware layer consisting of a flexure representing a flexible workpiece and an actuator that emulates the virtual cutting forces computed in the software layer. Controlled experiments on the HiL simulator agree with model predictions, and confirm an increase in the chatter vibration free cutting performance at low speeds in the presence of process damping. These results can instruct investigating other nonlinearities co-occurring with process damping to develop solutions to mitigate them.

**Keywords:** Turning, Process damping, Chatter, Hardware-in-the-loop simulator.

### 1. Introduction

Self-excited regenerative type chatter vibrations fundamentally limit the cutting performance capability of machine tool systems. Chatter occurs due to the interaction of cutting process with the machine tool dynamics, and when it occurs, it increases tool wear and may damage components of the machine tool. Models for chatter are hence very useful to prescribe ways to avoid it [1]. Models prescribe cutting at parameters that lie below the boundaries of stability. Sometimes, at low cutting speeds, experimental observations depart from model predictions that suggest a lower boundary than observed in practice [2]. The gain in stability limit at lower cutting speeds is usually attributed to the friction between the tool flank face and freshly cut surface, which adds process damping to the system [2]. The thrust force at the tool flank face acts against the relative vibration velocity of the tool-workpiece and purportedly induces damping in the cutting process [3]. Process damping is thought to depend on the amplitude and wavelength of vibrations and their complex relationship with vibration frequencies, cutting speeds, and tool wear [2-4].

Since process damping results in a preferential increase in the stability boundary at low speeds, different models have been proposed to characterize the main mechanisms responsible for improvement in cutting performance. Wallace and Andrew [3] helped reveal that process damping occurs due to the distribution of cutting forces over the contact zone between flank face and freshly cut surface. A detailed qualitative theoretical and experimental proof of stability with process damping was established by Sisson and Kegg [2]. An experimental technique was proposed in [4] to identify the dynamic cutting force coefficients responsible for process damping effects. Nice summaries of detailed theoretical and experimental investigation on process damping in turning and milling processes can be found in [4,5].

Although there exist models that characterize process damping and though some of these models can guide experimentation, efficacy of most of the existing models is prevaricated by the complex relationship between the amplitude and wavelength of vibrations, vibration frequencies, cutting speeds, and tool wear. Furthermore, since chatter increases tool wear, and since this relationship is also not well defined, experiments to confirm the increase in the stability boundary at low cutting speeds in the presence of process damping can sometimes be difficult to perform. In this light, this paper offers an alternate and controlled way of investigating the effects of process damping in cutting processes. We suggest the use of a hardware-in-the-loop (HiL) simulator that has hardware and software layers in which sensors and actuators are used to emulate the physics of the cutting process in the presence of process damping. Since cutting is only emulated on the HiL simulator, vagaries of uncertainties due to tool wear are avoided, and the platform allows for controlled investigations of complex cutting behavior.

HiL simulators have been successfully used previously to study stability of turning [6–12] and milling processes [13,14]. HiL simulators have also been used to test different active damping control strategies to mitigate machine tool vibrations [6,8,11–13]. Though the stability of the cutting processes and measures to control vibrations have been successfully emulated on HiL simulators, emulating chatter in turning with process damping has not been reported in the literature. As such, emulations presented in this paper are new, and is our modest claim to a contribution to state of the art. Emulating such phenomenon can be instructive for the investigations of process damping co-occurring with nonlinear cutting force characteristics in other cutting processes, and in developing active damping solutions to mitigate them.

The rest of the paper is structured as follows: at first, the mechanical model of the turning process with process damping is presented in Section 2. This section also discusses the method of solution for stability using the semi-discretization method [15]. A brief description of the HiL simulator for turning process is described in Section 3. In Section 4, a discussion on validation of the HiL simulator for linear cutting force characteristics while neglecting process damping effect is presented. The results of emulated stability with process damping in turning are discussed in Section 5, followed by the main conclusions of the present work.

## 2. Mechanical model of turning with process damping

The mechanical model of a turning process with process damping is shown in Fig. 1. We assume the tool is rigid and the workpiece is flexible, and that it can be approximated as a single degree of freedom system. The flank face of the tool interfering with the cut surface and contributing to the process damping phenomenon is also shown in Fig. 1.

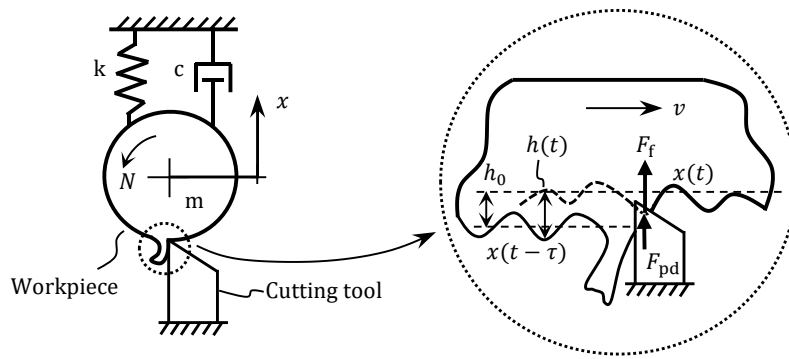


**Fig. 1.** Mechanical model of turning process with process damping; the inset shows the variation in chip thickness due to regenerative effect along with interference of the tool flank and machined surface.

From Fig. 1, the resulting governing equation of motion representing turning process dynamics can be written as:

$$\ddot{x}(t) + 2\zeta\omega_n\dot{x}(t) + \omega_n^2x(t) = \frac{F_f(t) + F_{pd}(t)}{m}, \quad (1)$$

wherein,  $m$ ,  $\zeta$  and  $\omega_n$  are the mass, damping ratio, and natural frequency of the workpiece.  $F_f(t)$  is the cutting force in feed direction which is assumed to be linear in the present case, i.e.,  $F_f(t) = K_f b h(t)$ , in which  $K_f$  is the empirically identified cutting force coefficient,  $b$  is the depth of cut and  $h(t) = h_0 + x(t - \tau) - x(t)$  is the total chip thickness.  $h_0$  is the mean chip thickness,  $x(t)$  and  $x(t - \tau)$  are the vibration amplitudes corresponding to the present and the previous revolutions, respectively.  $\tau = 60/N$  is the spindle period, also known as regenerative delay and  $N$  is the spindle speed in rpm. During machining, the tool/workpiece gets excited due to cutting forces and relative vibrations between tool and workpiece may become large, which may lead to an instantaneous loss of contact of the tool with the workpiece [16]. Due to the tool jumping out of cut phenomenon, the regenerative effects do not only depend on just the previous revolution but also multiple previous revolutions vibration data, and the expression for the total chip thickness will hence become  $h(t) = x_{\min} - x(t)$ , wherein,  $x_{\min}$  is the

smallest value of  $\{h_0 + x(t - \tau), 2h_0 + x(t - 2\tau), \dots\}$  taken over several previous revolutions.

$F_{pd}$  in Eq. (1) is the process damping force. For analysis herein, we assume it takes the form suggested in [4], i.e.,  $F_{pd}(t) = -Cb\dot{x}(t)/v$ , in which  $C$  is the velocity dependent cutting force coefficient and  $v$  is the cutting speed. The process damping force is vibration velocity proportional, and since this velocity is related to the frequency ( $\omega$ ), wavelength ( $\lambda$ ), and cutting velocity ( $v = \frac{\omega}{2\pi} \times \lambda$ ), the process damping force also depends on these parameters. Furthermore, since the cutting speed is a function of the diameter ( $d$ ) of the workpiece being cut ( $v = \pi dN/60$ ), process damping forces increase with a reduction in the spindle speed and workpiece diameter, which ultimately increases the stability limit at low spindle speed. Moreover, since these forces oppose the motion of the cutting tool, it is to be subtracted from the cutting force resulting from chip formation.

On substituting the expressions of  $F_f(t)$  and  $F_{pd}(t)$  in Eq. (1), the governing equation of motion forms a delay differential equation (DDE). The DDE with process damping can be solved for stability using the Nyquist frequency domain [4] or the time domain [5] or using the semi-discretization method (SDM) [15].

We use the well-established SDM due to its robustness in handling nonlinearities in the cutting process. For solving Eq. (1) using SDM, it is converted into state-space form as:

$$\dot{\mathbf{x}}(t) = \mathbf{A}(t)\mathbf{x}(t) + \mathbf{B}(t)\mathbf{x}(t - \tau), \quad (2)$$

$$\text{wherein } \mathbf{A}(t) = \begin{bmatrix} 0 & 1 \\ -\left(\omega_n^2 + \frac{K_{fb}}{m}\right) & -\left(2\zeta\omega_n + \frac{Cb}{mv}\right) \end{bmatrix}, \mathbf{B}(t) = \begin{bmatrix} 0 & 0 \\ \frac{K_{fb}}{m} & 0 \end{bmatrix}.$$

In SDM, the stability of the cutting process is obtained by determining the Eigenvalue of the transition matrix from Eq. (2) [15]. The limiting stability condition is established when the modulus of Eigenvalue is unity. Using this condition, a theoretical stability chart is constructed by scanning different values of depth of cut for the spindle speed range of interest. The stability chart without process damping can be constructed by simply putting  $C = 0$  in Eq. (2).

### 3. Hardware-in-the-loop simulator

The hardware-in-the-loop (HiL) simulator consists of a hardware layer and a software layer as shown in Fig. 2. The HiL simulator used herein has been built and reported in our previous work [11,12], wherein the characteristics of the key components of the HiL simulator have been detailed.

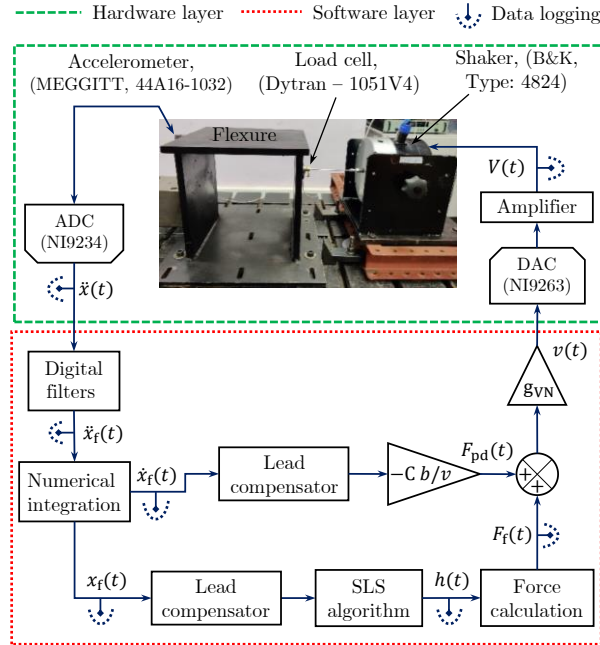


**Fig. 2.** Block diagram of the hardware-in-the-loop simulator for turning process with process damping.

The hardware layer contains a flexure that represents a flexible workpiece and a shaker that emulates the cutting force onto the flexure. The shaker has a force capacity of 100 N, which is connected to the flexure via a stinger. A load cell and an accelerometer are mounted on the flexure to monitor input force and output response, respectively. The hardware layer also includes a cRIO-9036 controller with an onboard FPGA module and plugged-in analog to digital converter (ADC) and digital to analog converter (DAC). The software layer has been programmed in NI-LabVIEW 2018, which includes data acquisition, filtering, numerical integration, calculation of regenerative cutting forces, and process damping forces. It also includes a surface location storage (SLS) algorithm that incorporates tool jumping out of cut and multiple regenerative effects [12].

The total delay in the mechatronic HiL simulator is estimated based on the method suggested in [11] and compensated using a phase lead compensator in the software layer, see Fig. 2. The modal parameters of the flexure coupled with the shaker are:  $m = 12.98$  kg,  $c = 119.4$  Ns/m,  $k = 7.15 \times 10^6$  N/m and  $f_n = 118.1$  Hz. The calculated total cutting force, i.e., the sum of regenerative cutting force and process damping force, is converted into voltage by multiplying it with a voltage-to-force gain of the shaker ( $g_{vN} = 0.038$  V/N), and then transferred it to the shaker through its power amplifier.

#### 4. Validation of HiL simulator for a linear force model

The HiL simulator is validated for the orthogonal turning process without process damping effect ( $C = 0$ ). We assume a cold-rolled AISI1045 steel workpiece and carbide grooving tool (edge width – 2.4 mm, rake angle -  $0^\circ$ , clearance angle -  $7^\circ$ ) with linear cutting force characteristics,  $K_f = 1384 \text{ N/mm}^2$  [4]. For finding experimental critical stability points using the HiL simulator, we increase the depth of cut ( $b$ ) in steps of  $5 \mu\text{m}$  at a specified spindle speed ( $N$ ) and mean chip thickness ( $h_0$ ). The measured cutting force and displacement response for representative cases of stable and unstable are shown in Fig. 3.

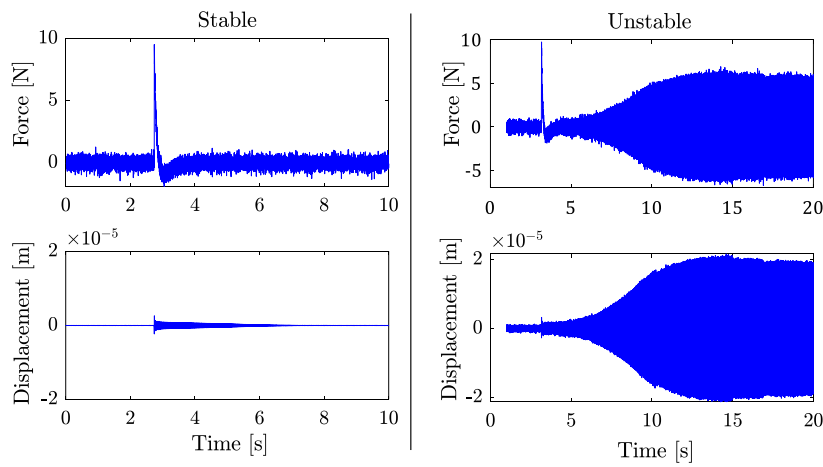


**Fig. 3.** Theoretical and experimental time domain response for stable ( $N = 2600 \text{ rpm}$  and  $b = 0.05 \text{ mm}$ ) and unstable case ( $N = 2600 \text{ rpm}$  and  $b = 0.15 \text{ mm}$ ).

Initially, for a particular combination of speed, depth of cut, and mean chip thickness ( $N, b, h_0$ ), the flexure is perturbed due to the static component of virtual cutting force ( $K_f b h_0$ ), if the response starts decaying with time, the cut is deemed stable, see Fig. 3. If the response starts to grow with time and whenever the first tool out of cut is detected, then the cut is considered unstable, and corresponding  $N, b$  and oscillation frequency are recorded for that case. In this way, experiments are conducted for spindle speed range of interest, see Fig 4.

It is clear from Fig. 4 that experimentally obtained stability behaviour is different from the model prediction. Such differences are also observed in earlier reported work [8,11] and are mainly attributed to delay in the mechatronic HiL simulator. Hence, the delay is systematically identified by the method suggested in [11] and is found to be  $\sim 0.8 \text{ ms}$ . Since the delay in the HiL simulator is equivalent to the negative phase, a phase lead compensator is designed and compensated suitably. The transfer function of the phase lead compensator is given below:

$$C(s) = \frac{8.07 \times 10^8 \left[ \left( \frac{s}{254.2} \right)^2 + 0.7 \left( \frac{s}{254.2} \right) + 1 \right]}{(s + 2)(s + 1457.5)(s + 5314.1)} \quad (3)$$

Eq. (3) is implemented in the software layer, see Fig. 2, and we repeated the chatter experiments with the compensator. The experimental procedure for finding stability points with a compensator is the same as those discussed without a compensator. The experimentally identified stability behaviour with the compensator is overlaid with the model prediction as shown in Fig. 4.

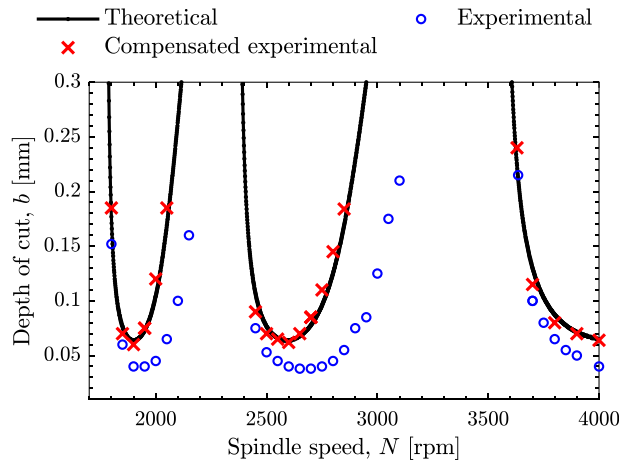


**Fig. 4.** Theoretical and experimental stability results with and without compensation of delay.

As is evident from Fig. 4, the experimentally observed stability behaviour on the HiL simulator with delay compensated system matches up well with the theoretically predicted stability boundaries, whereas, for the case of the delay not being compensated, the experiments diverge from prediction. Having validated the HiL simulator for the orthogonal turning process with linear force model, process damping phenomenon is introduced in the HiL simulator and experiments with those are discussed next.

## 5. Emulating stability with process damping

All analysis presented hereafter is for the case of the HiL with the delay compensated. Experiments on the HiL simulator are performed with process damping and for assumed linear cutting force characteristics. For the tool and workpiece material under consideration, the process damping coefficient is taken to be  $C = 10^6$  N/m and, the workpiece diameter was assumed to be 35 mm. If the tool geometry and/or workpiece material change, the coefficients ( $K_f$  and  $C$ ) will change accordingly. Vibration velocities necessary to calculate the process damping forces were obtained by numerically

integrating the accelerometer signal. Experimentally obtained stability along with theoretical results with process damping effect are shown in Fig. 5. Since process damping is generally a low-speed phenomenon, results shown in Fig. 5 are limited to the low-speed range of 500 – 1200 rpm.

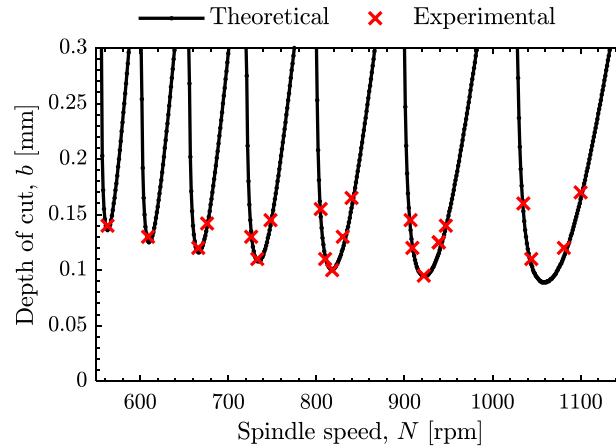


**Fig. 5.** Theoretical and emulated experimental stability behaviour with process damping.

As is evident from Fig. 5, the stability boundary at lower speeds is higher than at relatively higher speeds, and that experiments on the HiL simulator can closely capture modelled behaviour. These findings are consistent with earlier reported cutting experimental results [2,4], and demonstrates how the HiL simulator can also prove effective to investigate process damping related stability characteristics. Performing real cutting experiments at low spindle speed requires high torque at a given power rating of a spindle motor. Hence, investigation of process damping with different tool geometries and workpiece materials, workpiece diameter, and nonlinear force models on the real machine are difficult and not safe. These can easily be investigated on the present HiL simulator. Though present work focuses on the emulation of regenerative chatter with process damping on the HiL simulator, above mentioned other investigations will be part of future studies.

## 6. Conclusions

The stability of orthogonal turning process with process damping phenomenon that is prevalent in the real cutting process is experimentally emulated using a validated hardware-in-the-loop simulator. We show that experimentally emulated stability behaviour is in good agreement with the model predictions. Results reveal that stability limits with process damping at lower spindle speeds are higher than at higher spindle speeds and that these observations are consistent with the other earlier reported experimental works. Since the HiL simulator is non-destructive, it offers a cost-effective, repeatable, safe, and pedagogical tool for controlled experiments. Moreover, since it allows for

experiments while not suffering from the vagaries of uncertainties due to tool wear, it facilitates further analysis to characterize the complex process damping phenomenon. Though emulations herein discussed stability in turning in the presence of process damping for the case of a linear force model and for a defined process damping coefficient and workpiece diameter, other similar investigations to understand the role of the damping coefficient, workpiece diameter, and other force model types are possible, and can be as easily emulated on the HiL simulator.

## References

1. Altintas, Y., Weck, M.: Chatter stability of metal cutting and grinding. *CIRP Ann - Manuf Technol*, 53:619–42 (2004).
2. Sisson, T.R., Kegg, R.L.: An explanation of low-speed chatter effects. *J Eng Ind*, 91:951–8 (1969).
3. Wallace, P.W., Andrew, C.: Machining forces: some effects of tool vibration. *J Mech Eng Sci*, 7:152–62 (1965).
4. Eynian, M.: Chatter stability of turning and milling with process damping. PhD Thesis, The University Of British Columbia, (2010).
5. Saleh, K.: Modeling and analysis of chatter mitigatio strategies in milling. PhD Thesis, The University Of Sheffield, (2013).
6. Ganguli, A., Deraemaeker, A., Horodinca, M., Preumont, A.: Active damping of chatter in machine tools - demonstration with a “hardware in the loop” simulator. *J Syst Control Eng*, 219:359–69 (2005).
7. Matsubara, A., Tsujimoto, S., Kono, D.: Evaluation of dynamic stiffness of machine tool spindle by non-contact excitation tests. *CIRP Ann - Manuf Technol*, 64:365–8 (2015).
8. Mancisidor, I., Beudaert, X., Etxebarria, A., Barcena, R., Munoa, J., Jugo, J.: Hardware-in-the-loop simulator for stability study in orthogonal cutting. *Control Eng Pract*, 44:31–44 (2015).
9. Stepan, G., Beri, B., Miklos, A., Wohlfart, R., Bachrathy, D., Porempovics, G., et al.: On stability of emulated turning processes in HIL environment. *CIRP Ann - Manuf Technol*, 4–7, (2019).
10. Beri, B., Miklos, A., Takacs, D., Stepan, G.: Nonlinearities of hardware-in-the-loop environment affecting turning process emulation. *Int J Mach Tools Manuf*, 03611 (2020).
11. Sahu, G.N., Vashisht, S., Wahi, P., Law, M.: Validation of a hardware-in-the-loop simulator for investigating and actively damping regenerative chatter in orthogonal cutting. *CIRP J Manuf Sci Technol*, 29:115–29 (2020).
12. Sahu, G.N., Jain, P., Wahi P, Law M.: Emulating bistabilities in turning to devise gain tuning strategies to actively damp them using a hardware-in-the-loop simulator. *CIRP J Manuf Sci Technol*, 32:120–31 (2021).
13. Ganguli, A., Deraemaeker, A., Romanescu, I., Horodinca, M., Preumont, A.: Simulation and active control of chatter in milling via a mechatronic simulator. *J Vib Control*, 12:817–48 (2006).
14. Miklos, A., Takacs, D., Toth, A., Wohlfart, R., Porempovics, G., Molnar, T.G. et al.: The development of high speed virtual milling test. *Proc. ASME 2017 Dyn. Syst. Control Conf. DSCC2017 Oct. 11-13, 2017, Tysons, Virginia, USA*, p. 1–10 (2017).
15. Insuperger, T., Stépan G.: Updated semi-discretization method for periodic delay-differential equations with discrete delay. *Int J Numer Methods Eng*, 141:117–41 (2004).

10

16. Tlustý, J, Ismail, F.: Basic Non-Linearity in Machining Chatter Chatter. CIRP Ann - Manuf Technol, 30:299–304 (1984).

### **Acknowledgements**

This work was supported by the Government of India's Impacting Research Innovation and Technology (IMPRINT) initiative through project number IMPRINT 5509.